Overview of Impurity Control and Wall Conditioning in NSTX

H.W. Kugel[a], R. Maingi[b], M. Bell[a], W. Blanchard[a], D. Gates[a], D. Johnson[a], R. Kaita[a], S. Kaye[a], R. Maqueda[c], J. Menard[a], D. Mueller[a], M. Ono[a], Y-K. M. Peng[b], R. Raman[a], A. Ramsey[a], A. Roquemore[a], C. Skinner[a], S.Sabbagh[e], D. Stutman[f], W. Wampler[g], J. R. Wilson[a], S. Zweben[a], and the NSTX National Research Team

[a]*Princeton Plasma Physics Laboratory, Princeton University, Princeton, NJ 08543, USA.*

[b]*Oak Ridge National Laboratory, Oak Ridge TN, 37831 , USA*

[c] *Los Alamos National Laboratory, Los Alamos, NM, 87545, USA*

[d]*University of Washington, Seattle, WA, 98195, USA*

[e]*Columbia University, New York, NY, 10027, USA*

[f]*Johns Hopkins University, Baltimore, MD 21218, USA*

[g]*Sandia National Laboratories, Albuquerque, NM, 87123, USA*

Abstract

The National Spherical Torus Experiment (NSTX) started plasma operations in February 1999, and promptly achieved high current, inner wall limited, double null, and single null plasma discharges, initial Coaxial Helicity Injection, and High Harmonic Fast Wave results. NSTX is designed to study the physics of Spherical Tori (ST) in a device that can produce non-inductively sustained high-ß discharges in the 1 MA regime and to explore approaches toward a small, economical high power density ST reactor core. As expected, discharge reproducibility and performance were strongly affected by wall conditions. In this paper, we describe the internal geometry, and initial plasma discharge, impurity control, wall conditioning, erosion, and deposition results.

DISCLAIMER

DISCLAIMER

Portions of this document may be illegible in electronic image products. Images are produced from the best available original document.

1. Introduction

In February 1999, the National Spherical Torus Experiment (NSTX) achieved first plasma, and then, in a prompt manner indicative of a very robust design, achieved high current, inner wall limited, double null, and single null plasma discharges, initial non inductive current generation using Coaxial Helicity Injection (CHI), and High Harmonic Fast Wave (HHFW) results. Additional subsytems to be commissioned in CY 2000 include Neutral Beam heating, full graphite armor coverage, upgraded bakeout capability, boronization, and additional diagnostic systems.

This start-up was the first step in an investigation of the physics principles of low-aspect-ratio Spherical Tori (ST) in a device designed to study non-inductive start-up, current sustainment and profile control, confinement and transport, pressure limits and self driven currents, stability and disruption resilience, and unique scrape-off layer (SOL) and divertor characteristics.[1,2] These ST principles will be studied in regimes with high temperature, high density, non-inductively sustained high-β_T discharges ($\simeq$ 40%) with high pressure driven current fractions ($\simeq$ 70%) which could provide possible approaches toward a small, economic, high power ST reactor core.[2]

Fig.1 shows a partial schematic cross section of NSTX. The device capabilities include R_0 = 0.85 m, a = 0.67 m, R/a $\geq$ 1.26, κ = 2.2, δ < 0.5, I_p = 1 MA, B_T = 0.3T, a 5 sec maximum pulse length, copper Passive Stabilzer Plates, graphite power handling surfaces, 5 MW of Neutral Beam heating, 6 MW of 30 Mhz High Harmonic Fast Wave (HHFW) for heating and current drive at 10-20 w_{ICRF}. The 0.2 m radius Center Column is clad with alternating vertical columns of 1.3 cm thick ATJ graphite tiles between columns of Allied Signal (Type 865-19-4) 2-D Carbon Fiber Composite (CFC) tiles. The Inner Divertor tiles are 5.1 cm thick ATJ graphite; the Outer Divertor and Passive Stabilizer Plate tiles are 2.5 cm thick ATJ graphite. Shown in Fig.1, and in more detail in Fig.2, is a unique feature of NSTX: toroidal ceramic insulators, in the top and bottom Divertor gaps, for electrically biasing the inner and outer vessel for CHI. This configuration enables experiments with Ohmic, Neutral Beam and HHFW heated

discharges on Wall Limiter start-up plasmas, Lower Single-Null diverted plasmas, and Double Null diverted plasmas with and without CHI.

2. NSTX Boundary Physics, Power Deposition, and Wall Conditions

NSTX is expected to encounter plasma boundary regimes and plasma surface interactions similar to tokamaks but with significant differences. Fig.3 shows how the ST magnetic field line geometry differs from that of a conventional large aspect ratio tokamak. The inboard plasma side is dominated by the toroidal field, while the outboard plasma side is dominated by a strong poloidal field component. This magnetic geometry results in an ST outboard plasma edge characterized by a short field line of weak curvature and high pitch angle, and an inboard plasma edge characterized by a long field line of strong curvature and low pitch angle. The dominant good field curvature of the inner region provides the ST with MHD stability at high plasma pressure in reduced magnetic field (high-β). [2]

Another consequence of the ST magnetic geometry shown in Fig.3 is that in inner-wall limited discharges, the field in the Scrape-Off Layer (SOL) varies by a factor of 4 and in diverted discharges by a factor of 2. This results in a reflected and trapped ion flux in the SOL approaching 75% for inner wall limited discharges and 90% for diverted discharges. This reflection of trapped ion flux increases the effective parallel connection length in a collisionless edge plasma. Collisions reduce the effect of this trapping. Since the SOL is determined by the ratio of the parallel to perpendicular transport, the longer parallel connection length may cause a larger SOL in the ST as the edge plasma becomes less collisional. However, during Neutral Beam heating, under some conditions (*e.g.,* lower I_p), substantial ion loss may occur from large ion orbits in the outer region of bad curvature which could increase the perpendicular transport and tend to shortened the SOL. In addition, on inner wall surfaces, flux expansion ratios of ~10 in the SOL for ST Inner Wall Limited discharges will lower the effective incident power densities. In the outer region, however, the field line pitch of about 45° results in an short outer connection length from the midplane to the inner wall, and even shorter to the divertor plates for diverted discharges.

In NSTX, due the low aspect ratio, the tokamak divertor figure of merit "P/R", the ratio of heating power to major radius, commonly used to compare devices of comparable cross-field transport and magnetic flux expansion, will be ~2x that of tokamaks of comparable heating power. However, the effect of smaller major radius may be offset by effects discussed above which increase the power flux width. In HHFW heated discharges up to 6 MW for pulse lengths of 5 sec , the ratio P/R = 7.2 W/m and at the Separatrix P/A_{sep} = 0.2 MW/cm^2. When 5 MW NBI heated discharges are added, the peak injected powers approach ~11 MW and P/R~12 MW/m. In the initial NSTX operational phase, a maximum of 6 MW heating power will be applied. Simulations indicate [3,4] that the incident power densities on the divertor plates of Inner Wall Limiter discharges will be in the range 2.1 to 3.8 MW/cm^2. Similarly, the incident power densities on the divertor plates for Double Null Diverted discharges will be in the range 4.4 to 7.2 MW/m^2. Thermal response calculations [3,4] for the actively cooled, divertor tile, front face surface temperature rise indicate a peak temperature of 1200°C during a 5 sec application of the highest estimated power density of 7.2 MW/m^2. In the case of the Center Column, for a midplane profile-peaking factor approaching 2, the peak incident power density for Inner Wall Limited discharges is ~2MW/m^2. In the case of the Center Column tiles, which are not actively cooled, the expected tile front face surface temperature rise is $\leq$ 1000°C during a 5 sec application of an incident power density of 2 MW/m^2. Although these temperature rises are below the regime where radiation enhanced sublimation would instigate carbon blooms, this may no longer be the case as surfaces become micro-fractured and eroded due to intense ongoing ion bombardment. The application of additional heating power can be handled using shorter pulse lengths, but for longer discharges advanced heat-flux reduction techniques must be found.[2,3,4]

Discharge reproducibility and performance are expected to be strongly affected by wall conditions. The NSTX Experimental Plan calls for developing techniques and measures for establishing stable and reproducible plasma conditions for the duration of each specific experiment. These include bakeout of the armor tiles to 350°C, He Glow

Discharge Cleaning (GDC), and methods of deuterated boronization and lithiumization that can be applied before and during plasma operations. To date, a preliminary Bakeout system has been used to perform 3 bakeouts of the graphite and CFC tiles to increasing high temperatures; the last bakeout reached about 309°C on the Center Column and 220°C on the Passive Stabilzers. The final bakeout capability will allow heating all graphite and CFC tiles to 350 °C and the vacuum vessel to 150 °C. HeGDC has been performed routinely between selected discharges. A Solid target Boronization (STB) probe has been installed but not tested. Other boronization methods such as glow discharge aided chemical vapor deposition using deuterated boron compounds will be tested later. Hydrogenic boron compounds will not be used in NSTX due to the HHFW need to avoid a hydrogen parasitic resonance.

3. First Plasma Start-up With Preliminary Configuration

The initial configuration for first plasma start-up in February 1999 consisted of the stainless steel vacuum vessel, the Center Column partially clad (50%) with ATJ graphite, and a small ATJ graphite outer bumper limiter (*i.e.*, the Passive Stabiler Plates were not yet installed and no graphite on the Outer Divertors). The initial vessel evacuation started in mid November 1998. At that time the Bakeout System was not functional. In order to remove water, CO, CO_2, and hydrocarbons as rapidly as possible so as to meet the start-up schedule, about 39 hours of D_2GDC was performed at room temperature. This was followed by 4 hours of He GDC to remove residual D_2 and associated products. A preliminary GDC system was used for this process.[5] This consisted of a moveable 304-SS anode and a biased preionization filament for initiating GDC at the actual operating pressure and voltage [0.27 Pa (2mT) for D_2 and 0.53 Pa (4 mT) for He at 400V]. Starting at the actual operating pressure and voltage was done to reduce violent arcing and sputtering events, and to reduce stress on the torus vacuum pumping system which was kept in the normal high vacuum mode during GDC. Fig.4 shows a comparison of D_2GDC wall impurity cleaning followed by HeGDC wall conditioning to remove the residual D_2. It is seen that D_2GDC was very effective for removing impurities from the walls. HeGDC was found much less efficient for removing impurities but was found very effective for removing residual D_2. Fig.5 shows the

behavior of the base pressure as it approached about 2.7×10^{-9} Pa (2×10^{-8} T) by mid February 1999 after about 3 months pumping at 3300 l/s (D_2) at room temperature, and its subsequent behavior after First Plasma. The First Plasma discharge was limited to about 20 KA. Subsequently, the biased preionization filament was applied to assist plasma breakdown, and over a 1.5 day period, discharges were readily obtained up to 280 KA with about 1/3 of the available OH flux.

4. Restart in August 1999 After Additional Installations

After a 5 month vent to install additional hardware, NSTX was evacuated in early August 1999 with a nearly complete internal configuration (*i.e.*, as shown in Fig. 1) which included a divertor region clad 100% with graphite tiles, and copper Passive Stabilizer plates clad about 50% with graphite tiles. Other internal hardware installations included a double fixed anode GDC system with two biased filaments that allow GDC initiation at the operating pressure and voltage.[5] In view of the extensive construction that had taken place in the vessel during the 5 month vent, and the need to quickly remove residual impurities, about 140 hours of D_2GDC was performed at room temperature remove water, CO, CO_2, and hydrocarbons, and about 20 hours of HeGDC to remove residual D_2 and associated products. This was followed by a 206°C bakeout of the Center Column performed using resistive heating, during which 10 hours of D_2GDC and 12 hours of HeGDC were performed. In September 1999, operations resumed, and plasma discharges of over 800 KA were achieved relatively quickly. Two additional bakeout experiments were performed at increasing higher temperatures; during the last bakeout in November 1999, the Center Column was heated to 309 °C and the Passive Stabilizer to about 220°C. Fig.6 shows the vessel base pressure behavior and the partial pressures of the mass 18, 28, 32, and 44 impurity components.

During this work, the vessel windows were not shuttered, and the transmission of an exposed midplane window near a GDC wall anode was measured after GDC, bakeout, low Ohmic power plasma operations (Ip ~<500KA). The transmission in the visible was found to decrease about 5% per 10 hours of D_2 or He GDC at room temperature. Absolute measurements of an exposed window coating transmission in

the visible, RBS relative measurements of thickness and elemental composition indicated that the depositions prior to CHI and Ohmic discharges with Ip >0.5 MA was ~ <550å thick with the following composition: H (18.3%), C (15.0%), O (24.0%), Cr (5.5%), Fe (23.0%), Cu (12.0%), and Mo (0.20%). No deuterium was observed even though only deuterium plasmas were used (no hydrogen plasmas or GDC were ever used), hence, the hydrogen content is attributed to hydrogenic components from the wall outgassing. Relatively little carbon was observed even though there was an extensive graphite surface. The deposition appears to be mostly metal oxides. Visible window transmissions measured at other toroidal locations increased systematically as the distance from the GDC wall anodes increased indicating some enhanced local deposition near the GDC anodes.

5. Plasma Operation Results

The experimental campaign achieved about 1125 discharges, during 41 plasma operation days with nearly 30 discharges per day. After the final bakeout in November 1999, improved wall conditions and advances in control technique allowed higher current discharges to I_p > 0.9 MA for 70 ms (W_{tot} =31 kJ, β_t =5.6%, τ_e =15 ms), and by December 14, 1999, 1 MA discharges were attained with ramp-rates of 7 MA/sec.[6,7] Fig.7 shows the trend in peak plasma current attained as the campaign progressed. In these discharges, Electron Cyclotron Preionization (80 Ghz, 30 kW) and biased filament preionization was used routinely to assist discharge initiation. Plasma position was controlled in the feedback mode. Often early in the current rise phase, at ramp rates greater than about 5MA/sec, MHD activity occurred which exhibited coherent Mirnov oscillations of decreasing frequency indicative of possible locked tearing mode. In the flattop region, stored energy and plasma beta increased monotonically with plasma current. MHD, P_{rad}, soft x-ray, l_i evolution correlations were consistent with high core radiation indicating that some MHD events may have been radiation driven. Late in the discharge, Internal Reconnection Event (IRE) were often observed as the loop voltage decreased. In general, these initial results suggest that heating during the initial I_p ramp will be important for achieving longer pulse discharges.[7]

CHI discharges were obtained up to 130 KA with CHI injected currents of 20 KA for ~500V bias yielding current multiplications off 6-7. In some experiments, current multiplications up to 10 were obtained. Stable high current discharges were produced up to 130 ms for some discharges. CHI discharges were demonstrated with fast puff divertor region D_2 pressures from 2.1 Pa (16 mT) down to 0.13 Pa (1 mT). The CHI ceramic insulators in the divertor gaps performed satisfactorily through the campaign. However, evidence of arcing and depositions in the insulator regions suggested improvements for additional insulator protection and metallic impurity reduction.[8]

The RF antenna system was vacuum conditioned to 25kV. During plasma operations, good antenna plasma matching was achieved with 8 antennas and two transmitters, and a reactive shift with plasma edge location was observed. No significant parasitic loading was observed. 2 MW of HHFW power was injected into ohmic target plasmas, and an increase in plasma energy was observed. Soft x-ray spectra showed centrally peaked electron heating during a modulation experiment using 0-π-0-π phasing to yield the slowest phase velocity; other phasing did not exhibit heating, and this observed phase dependence is under investigation. HHFW antenna structures (*e.g.*, BN shields) perfomed well at 2 MW and in the edge plasmas of high current discharges.[9]

During ohmic operations, about 40 discharges were required to achieve low reproducible D_α edge light emission. In general, the application of HeGDC between discharges had no systematic impact on plasma recycling and plasma performance in the flat-top region. It was useful if the plasma had start-up problems. In special cases, for example, following initial CHI experiments, 30 minutes of HeGDC was performed, and it took 5-10 Single-Null discharges to reduce visible light emission back to pre-CHI levels. After this, performing 5 minutes of HeGDC between discharges made a step change (~10%) to achievable plasma current and/or flattop duration; subsequent 5 minute HeGDC between discharges exhibited no improvement in plasma performance. In other discharge sequences, the recycling/visible light baseline was reduced by only up to 10% after 3 HeGDC /plasma discharge sequences (Fig.8). The (H_α /H_α+D_α) ratio,

which is important to minimize in NSTX so as to avoid parasitic HHFW resonance, was about 95% before the October 1999 bakeout but reached less than 10% by the end of the campaign. Initial visible spectroscopic measurements indicated moderate levels of low-Z impurities that tended to increase with discharge number during a given operating day. Filtered soft-Xray measurements of plasma profiles indicated that metallic impurities due to exposed copper and stainless steel were often high.[10]

Initial measurements of microscopic edge turbulence were performed with a fast-framing camera (1000 Hz). An applied edge gas puff rendered visible, fast moving edge density turbulence "filaments" with a poloidal wavelength of 10 to 15cm (Fig. 9). These initial edge density turbulence may be characteristic of present operating conditions and will be used to characterize edge cross-field transport and frequency spectra in the boundary of various NSTX plasma regimes.[11]

Four stainless steel and two silicon sample coupons (2.5cm x 2.5cm) were mounted at the midplane at four toroidal locations on the outer vessel wall about 10cm beyond the SOL of the most outward plasma. In addition, 12 stainless steel coupons were positioned in a Poloidal Array at one toroidal location in a Passive Stabilizer gap, about 4cm beyond the major radius of the graphite tiles on the plasma facing side of the Passive Stabilzers. Each of the stainless steel coupons was partially coated with a 0.4μm layer of graphite so as to provide measurements of both deposition and erosion. Deuterium implanted from the plasma in the carbon of the coupons was consistent with saturation by particles of a few hundred eV.[12] The change in carbon thickness was measured using a 1.5 MeV proton RBS before and after plasma exposure.[12] The results indicate net carbon erosion of all coupons. In the case of the Poloidal Coupon Array, more carbon erosion occurred on the lower Passive Plate (0.17-0.25μm) than on the upper Passive Plate (0.02-0.1μm) coupons. In the case of the Toroidal Coupon Array, on the outer vessel wall, the carbon erosion varied from ~0.06μm to ~ 0.33μm.[12] This toroidal asymmetry is under investigation but may be related in part to the shadowing and reflection effects of nearby hardware. Erosion of wall coupons was also observed on JET and attributed to effect of charge exchange neutrals.[13] Metal

deposition (mainly Fe and Cu) was found on all coupons. In the case of the Poloidal Coupon Array, more metal was found on the lower Passive Stablizer coupons (~ 1.2-1.5x10^{17}/cm^2) than on the upper (~ 0.5x10^{17}/cm^2).[11] This asymmetry may be attributable to the effect of the first CHI plasma experiments which were initiated across the Lower Divertor gap region; Single Null Ohmic plasma discharges may have also contributed.

2 MeV ^{4}He RBS and Electron Microscopy were used to measure metal deposition on four lower Passive Plate graphite tiles.[12] Fe and Cu were observed in rough areas (local depressions) on the plasma facing surfaces at ~2x10^{17}/cm^2, similar to the metal coverage on the lower Passive Stabilizer coupons.

Center Column erosion was studied by implanting two Center Column tiles (one ATJ graphite and one Allied Signal CFC) with 300 keV Si to a depth of 0.34μm. Ion Beam analysis was performed before and after exposure to NSTX plasmas during the August 1999 Experimental Campaign. 2 MeV ^{4}He RBS measurements found the Si markers to be absent, thereby indicating net erosion exceeding >0.4μm. In addition, metallic deposition of 0.13x10^{17}/cm^2 was found on the graphite tile and 0.48x10^{17}/cm^2 on the CFC tile which is about 10x less metal than deposited on the outer wall coupons and passive plate tiles.[12] This difference may be due to higher erosion rates on the Center Column than on outer coupons which were more distant from the plasma edge.

There was no macroscopic damage to the ATJ graphite tiles of the Center Column, Inner and Outer Divertors, and the Passive Plates other than symmetric discoloration on plasma-facing, power-absorbing surfaces and a few arc spots. In general, the visible changes to these plasma facing surfaces were toroidally symmetric but different for the Lower and Upper Divertors. The Lower Outer Divertor exhibited thermal deposition pattern extending from the divertor gap to its major radius center, however, the Upper Outer Divertor tile surfaces exhibited a more centralized thermal deposition pattern. The Upper Divertor pattern may be indicative of normal Double Null Ohmic plasma depositions, whereas the Lower Divertor pattern may be due to the sum

effects of Single Null plasmas, Double Null plasmas, and CHI startup across the Lower Divertor gap region.

In contrast to the ATJ graphite tile surface changes described above, the Allied Signal CFC tiles exhibited from about 2 to 8, horizontal damage or fracture tracks. These fracture tracks have the visual appearance of cracks but were actually shallow tracks about 0.1cm wide by 0.01 cm deep and varying in length from about 0.5cm to 3cm. Some fracture tracks are uniformly deep, others appear to be a series of pits. The axises of these fracture tracks seem parallel to the carbon fibers embedded in the CFC material. Indeed the tiles were machined so that the CFC fibers were oriented parallel to the plasma facing side. However, due the curvature the tile surface, fiber ends appear at the surface. These exposed ends of near surface fibers may have accelerated the expulsion of fibers. In addition, machining induced micro-stresses in thin layers covering near-surface fibers may have fractured under cyclic thermal stress. In the case of a typical fracture track size of 0.5cm long by 0.1cm wide by 0.01cm deep, a typical track volume of ~$5x10^{-4}$ /cm^3 would have released about 1 mg, or $5x10^{19}$ atoms of carbon into the plasma edge. This CFC behavior will be monitored during forthcoming NBI operations which will result in much higher power loading on these tiles.

The CHI ceramic insulators in the divertor gaps performed satisfactorily through the campaign. However, evidence of arcing and depositions in the insulator regions suggested improvements for additional insulator protection and metallic (Fe and Cu) impurity reduction.[8]

6. Conclusions

NSTX started plasma operations in February 1999. The relatively prompt manner in which NSTX achieved high current, inner wall limited, double null, and single null plasma discharges, initial Coaxial Helicity Injection, and High Harmonic Fast Wave results is indicative of a very robust design, and suggests that it can be used to study

ST principles in high performance regimes that could provide possible approaches toward a small, economic, high power ST reactor core.

Acknowledgments

We wish to acknowledge the technical contributions of M. Anderson, R. Cutler, T. Czeizinger, G. D'Amico, M. Dimattia, S. Edwards, R. Gernhardt, L. Guttadora, T. Holoman, T. Provost, J. Sorensen, J. Timberlake, J. Winston, and the NSTX support and operating Staffs. This work is supported by U. S. DoE contracts DE-AC02-76-CH0-3073 and DE-ACO4-94AL85000.

References

1. Y-K. M. Peng and D. Strickler, *Nucl. Fusion*, **26**, (1986) 769.
2. S.M. Kaye, *et al.*, *Fus. Technol.* **36**, (1999) 16, and references therein.
3. R. Maingi, *Proc. Int. Workshop ST's*, Abingdom, United Kingdom, 1996.
4. R. Maingi, *Proc. Int. Workshop ST's*, St. Petersburg, Russia, 1997.
5. H. W. Kugel, *et al.*, Proc. of the 18th Symposium On Fusion Engineering, Albuquerque, NM, October 25-29, 1999, (IEEE, 1999) 296.
6. M. Bell, *et al.*, Proc. of the European Physical Society Conference on Controlled Fusion and Plasma Physics, Budapest, Hungary, June 12-16, 2000.
7. J. Menard, *et al.*, Proc. of 18th IAEA Fusion Energy Conference, Sorrento, Italy, Oct.4-10, 2000.
8. R. Raman, *et al.*, Proc. of 18th IAEA Fusion Energy Conference, Sorrento, Italy, Oct.4-10, 2000.
9. J. R. Wilson, *et al.*, to be published.
10. D. Stutman, *et al.*, Bull. A. Phys. Soc. **44**(7), (1999) 187.
11. S. Zweben, *et al.*, Bull. A. Phys. Soc. **44**(7), (1999) 187.
12. W. Wampler, *et al.*, to be published.
13. M. Mayer, *et al.*, J. Nucl. Mater, **266-269** (1999) 604.

Figure Captions

Fig.1 Partial schematic cross section of the NSTX device.

Fig.2 Partial schematic of lower Divertor Gap showing the lower toroidal ceramic insulator (a similar insulator is in the upper Divertor Gap) for electrically biasing the inner and outer vessel for CHI.

Fig.3 Schematic of Spherical Torus (ST) magnetic field line geometry.

Fig.4 Comparison of D_2GDC impurity cleaning followed by HeGDC wall conditioning for February 1999 vessel configuration. D_2GDC was very effective for removing impurities from the walls. HeGDC was used to remove residual D_2.

Fig.5 Base pressure from Dec98 to Feb99 as D_2DGC and HeGDC were applied to prepare NSTX for First Plasma (refer to text).

Fig.6 Vessel base pressure behavior and the partial pressures of the mass 18, 28, 32, and 44 impurity components as walls were conditioned using D_2GDC, HeGDC, and bakeout to prepare NSTX for 1 MA Discharges.

Fig.7 The trend in peak plasma current attained as the campaign progressed. In these discharges, Electron Cyclotron Preionization (80 Ghz, 30 kW) and biased filament preionization was used routinely to assist discharge initiation.

Fig.8 Edge luminousity behavior of Da and HeII for HeGDC sequences (refer to text).

Fig.9 An applied edge gas puff rendered visible, fast moving edge density turbulence "filaments" with a poloidal wavelength of 10 to 15cm.

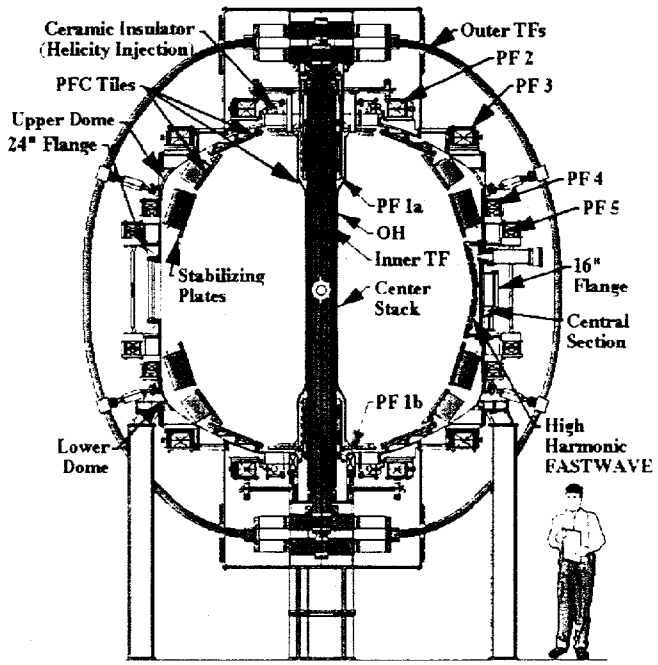

Fig.1 Partial schematic cross section of the NSTX device.

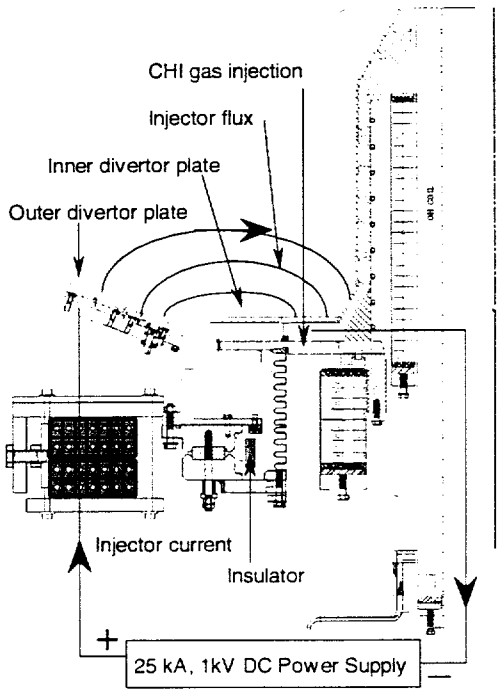

Fig.2 Partial schematic of Lower Divertor Gap region showing the lower toroidal ceramic insulator for electrically biasing the inner and outer vessel for CHI. A similar insulator is in the Upper Divertor Gap.

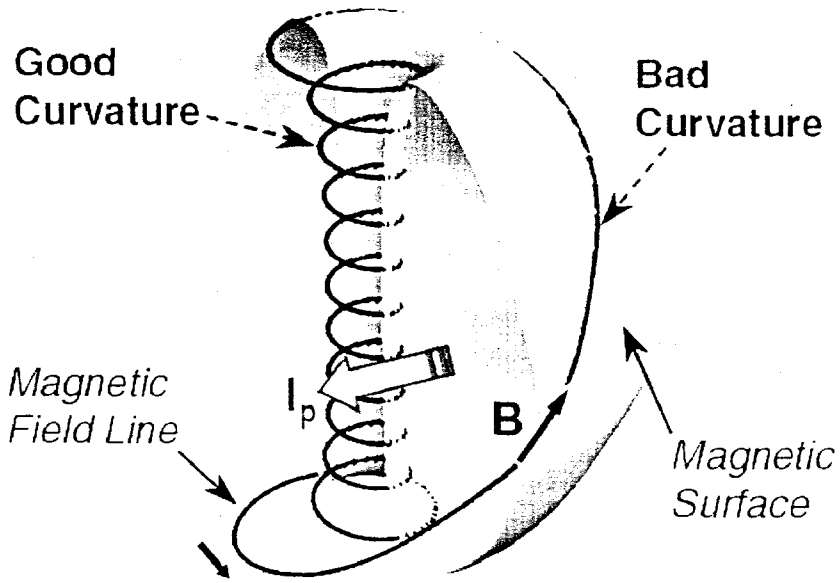

Fig.3 Schematic of Spherical Torus (ST) magnetic field line geometry.

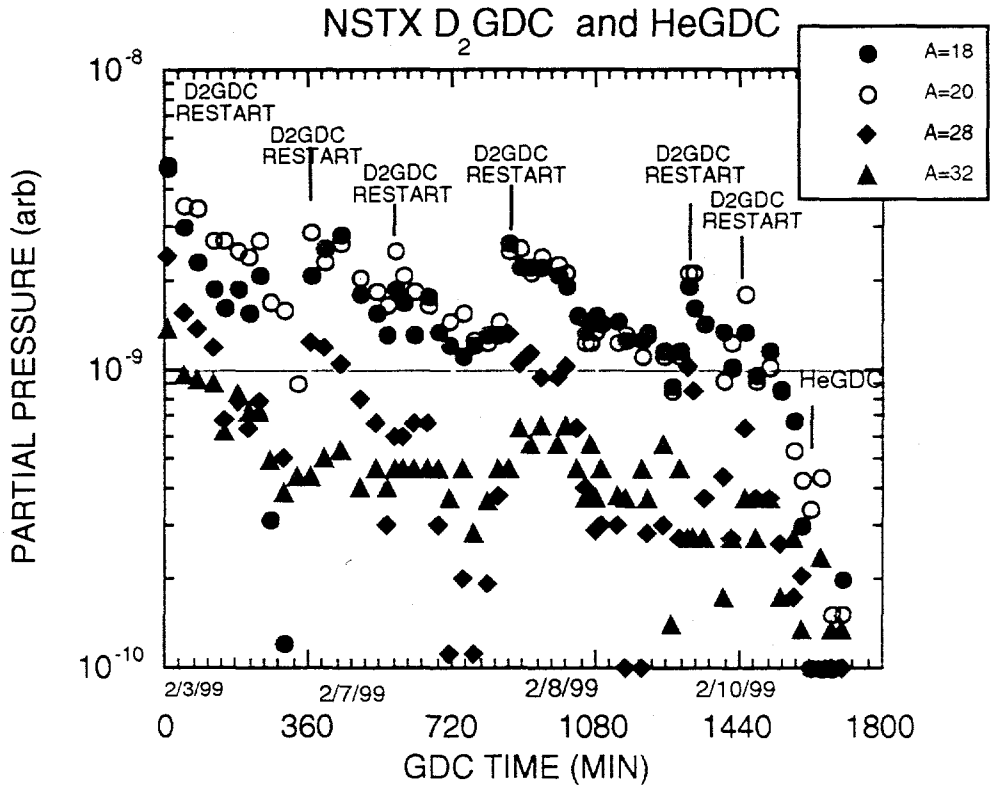

Fig.4 Comparison of D_2GDC impurity cleaning followed by HeGDC wall conditioning for February 1999 vessel configuration. D_2GDC was very effective for removing impurities from the walls. HeGDC was used to remove residual D_2.

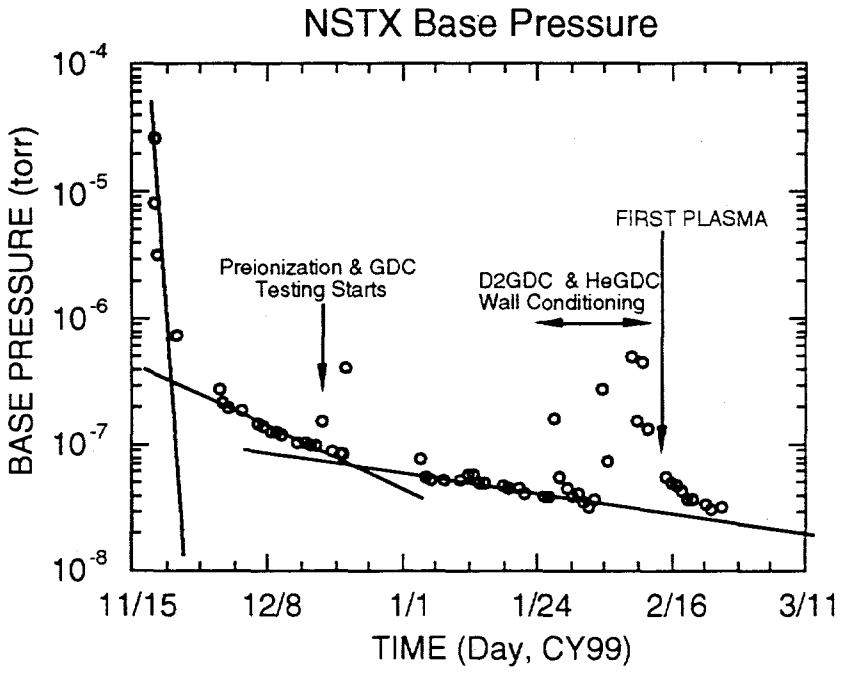

Fig.5 Base pressure from Dec98 to Feb99 as D_2DGC and HeGDC were applied to prepare NSTX for First Plasma (refer to text).

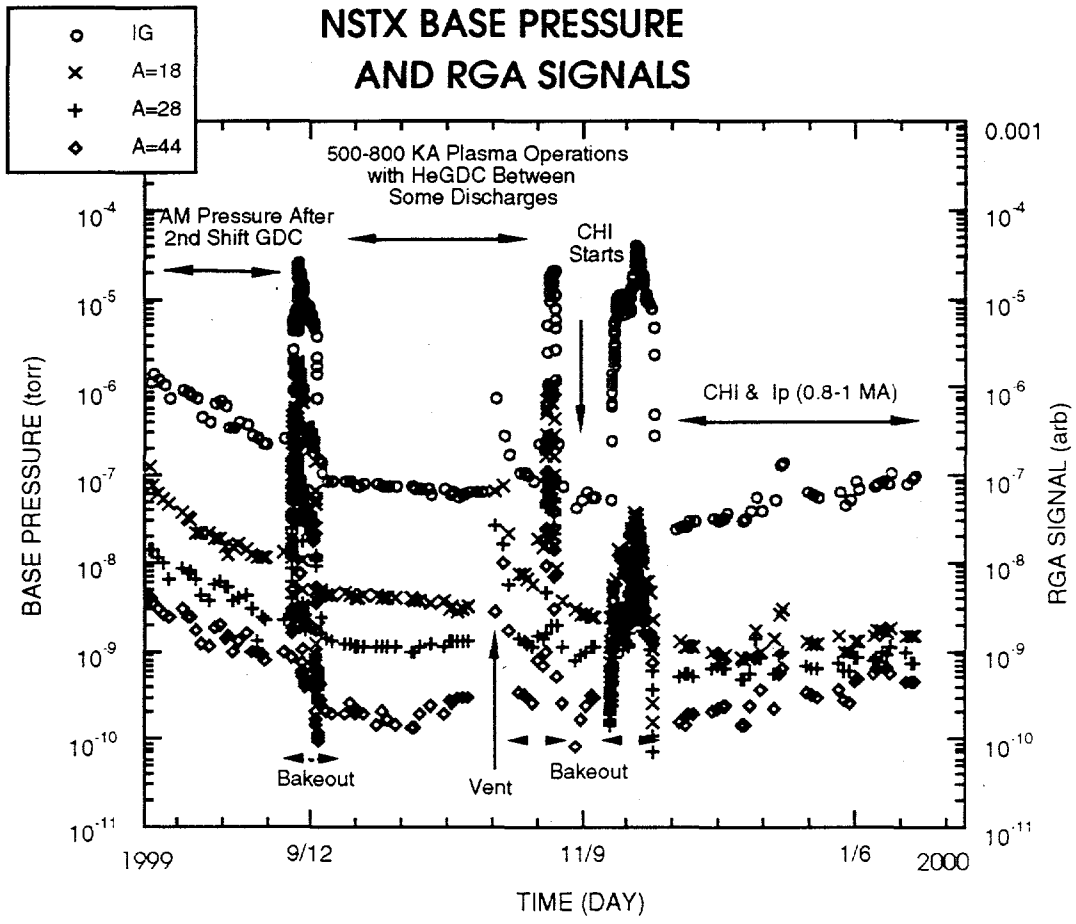

Fig.6 Vessel base pressure behavior and the partial pressures of the mass 18, 28, 32, and 44 impurity components as walls were conditioned using D_2GDC, HeGDC, and bakeout to prepare NSTX for 1 MA Discharges.

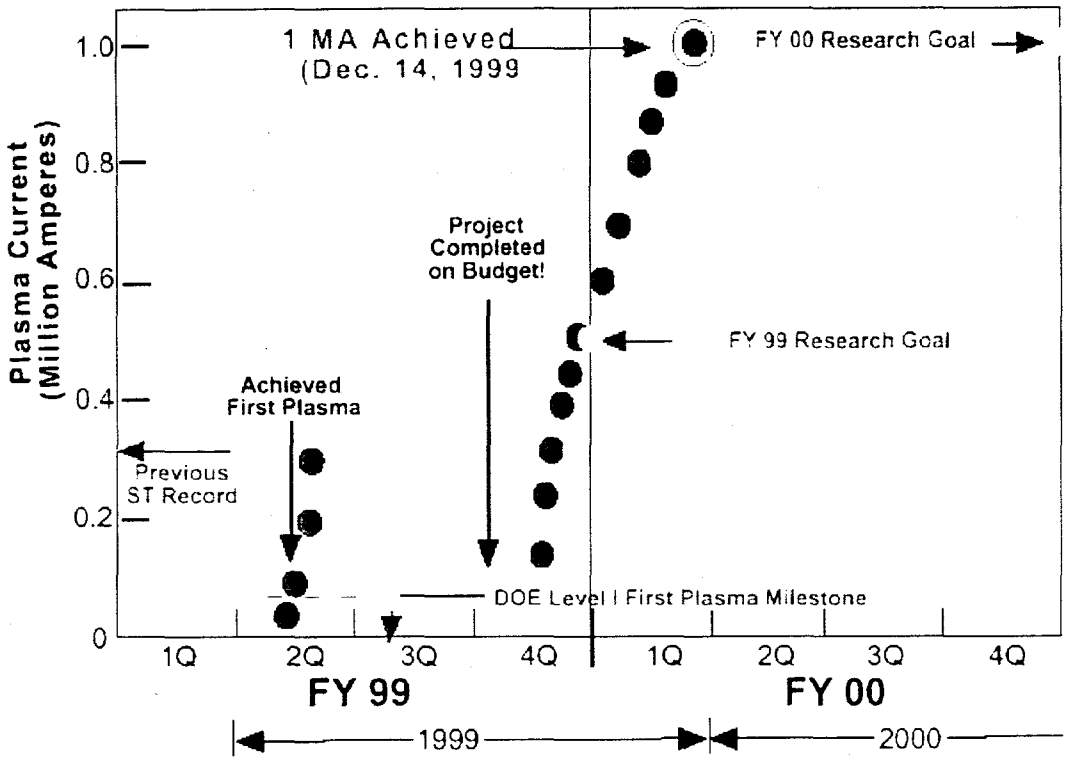

Fig.7 The trend in peak plasma current attained as the campaign progressed. In these discharges, Electron Cyclotron Preionization (80 Ghz, 30 kW) and biased filament preionization was used routinely to assist discharge initiation.

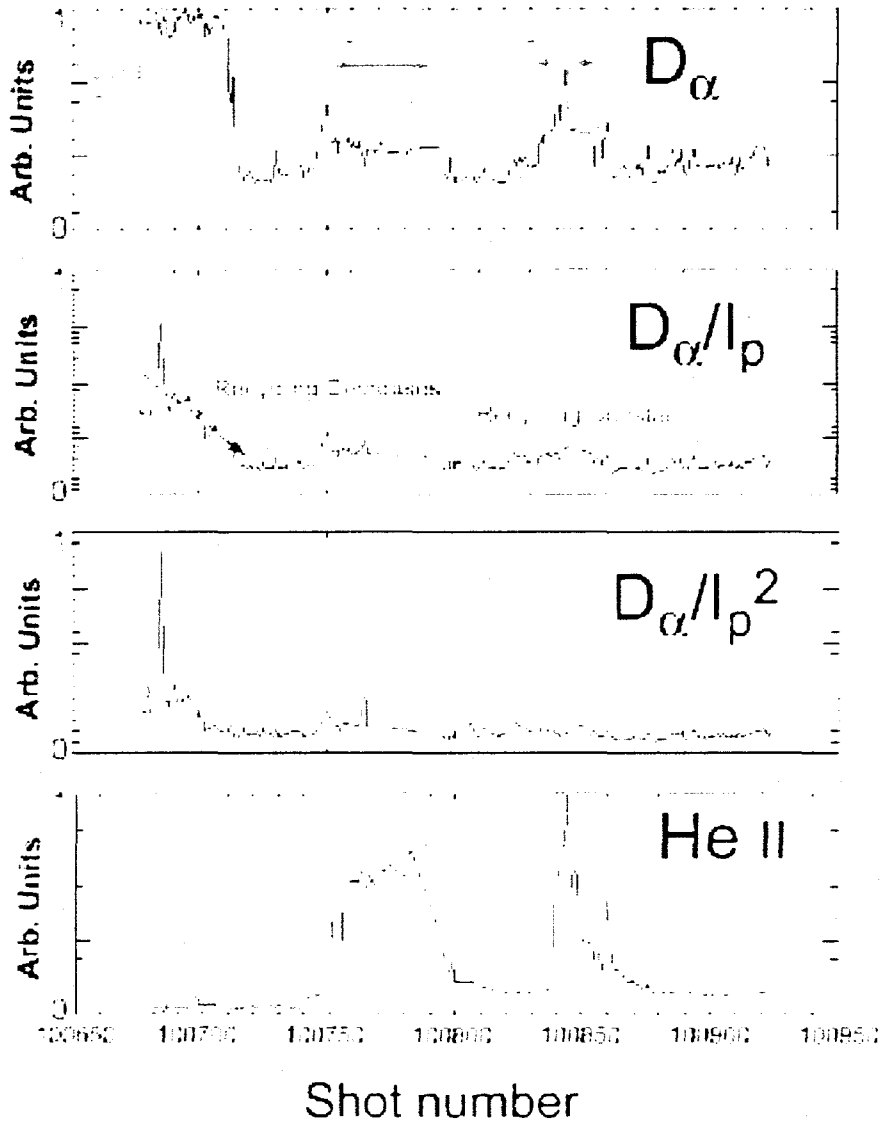

Fig.8 Edge luminousity behavior of Dα and HeII for HeGDC sequences (refer to text).

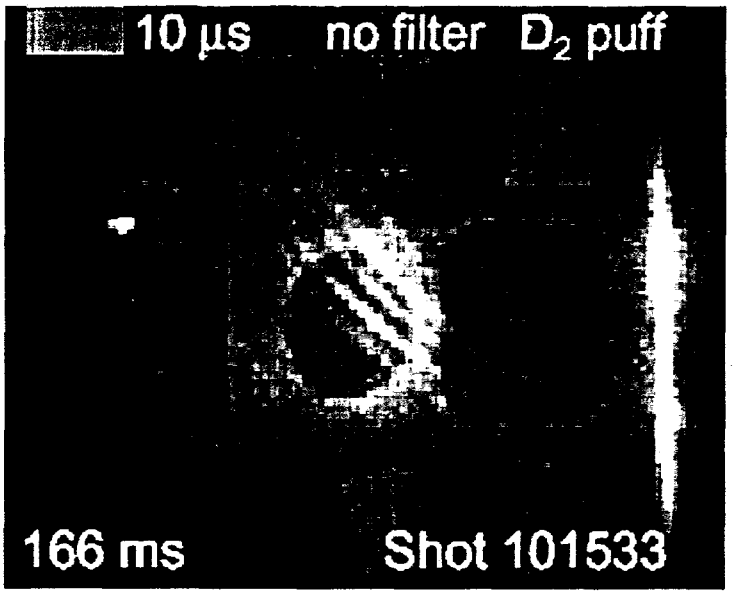

Fig.9 An applied edge gas puff rendered visible, fast moving edge density turbulence "filaments" with a poloidal wavelength of 10 to 15cm.